Fibrillar Layer as a Marker for Areas of Pronounced Corneal Endothelial Cell Loss in Advanced Fuchs Endothelial Corneal Dystrophy

AGATHE HRIBEK, THOMAS CLAHSEN, JENS HORSTMANN, SEBASTIAN SIEBELMANN, NIKLAS LORECK, LUDWIG M. HEINDL, BJÖRN O. BACHMANN, CLAUS CURSIEFEN, AND MARIO MATTHAEI

• PURPOSE: We sought to assess the correlation of corneal endothelial cell (CEC) density to alterations of collagen composition of Descemet membrane (DM) in advanced Fuchs endothelial corneal dystrophy (FECD) and to image such changes by slit-lamp biomicroscopy in vivo.

• DESIGN: Prospective, observational consecutive case series.

• METHODS: Fifty eyes (50 subjects) with advanced FECD were enrolled. After slit-lamp biomicroscopy and corneal Scheimpflug imaging, the Descemet endothelium complex (DEC) was retrieved during DM endothelial keratoplasty (DMEK) surgery. The expression of collagens I, III, and IV (COL I, COL III, and COL IV) and corresponding CEC density were analyzed by immunofluorescence flat mount-staining. Presence, diameter and surface area of collagen expression, and CEC density served as the main outcome measures.

• RESULTS: Immunofluorescence staining revealed central coherent collagen positive areas (mean surface area = 10 mm^2 ± 6 mm^2) corresponding to a fibrillar layer burying the guttae of DM in 84% (42/50) of DECs. CEC density overlying the fibrillar layer compared with the periphery was significantly reduced (−54.8%, $P < .0001$) with a steep decline of CEC density at its borders. Subgroup analysis revealed that the fibrillar layer may be imaged by slit-lamp biomicroscopy in vivo with significant positive correlation of mean maximum diameter detected by slit-lamp biomicroscopy ($d_{SL\ max}$ = 4.1 mm ± 0.9 mm) and by immunofluorescence staining ($d_{IF\ max}$ = 4.7 mm ± 1.1 mm; $r = 0.76$; $P = .001$).

• CONCLUSION: A fibrillar layer with a clear geographic pattern marks areas of pronounced loss of CEC density in advanced FECD eyes and may be imaged by slit-lamp biomicroscopy in vivo. (Am J Ophthalmol 2021;222:292–301. © 2020 Elsevier Inc. All rights reserved.)

AJO.com Supplemental Material available at AJO.com.

Accepted for publication Sep 14, 2020.

From the Department of Ophthalmology (A.H., T.C., J.H., S.S., N.L., L.M.H., B.O.B., C.C., M.M.) and the Center for Molecular Medicine Cologne (T.C., C.C.), University of Cologne, Faculty of Medicine and University Hospital Cologne, Cologne, Germany.

Inquiries to Mario Matthaei, Department of Ophthalmology, University Hospital of Cologne, Kerpener Str 62, 50924 Cologne, Germany; e-mail: mario.matthaei@uk-koeln.de

THE CORNEAL ENDOTHELIUM IS A MONOLAYER OF hexagonal corneal endothelial cells (CECs) that covers the inner stromal surface of the cornea. It maintains corneal deturgescence by a pump-leak mechanism. Fuchs endothelial corneal dystrophy (FECD) is a bilateral disease of the corneal endothelium characterized by an accelerated decrease of CEC density and subendothelial accumulation of extracellular matrix (ECM) starting at the corneal center and spreading toward the periphery.[1] Corneal endothelial dysfunction causes corneal edema with impaired visual acuity and pain in advanced stages of the disease.[1]

FECD is the most common indication for corneal transplant surgery (keratoplasty) worldwide and keratoplasty represents the only established treatment option.[2] Corneal transplantation has developed from penetrating keratoplasty over Descemet stripping automated endothelial keratoplasty (DSAEK) to Descemet membrane endothelial keratoplasty (DMEK).[2] DMEK generally replaces the central 8 mm of the diseased endothelium and provides excellent postoperative outcomes.[3] However, immune reaction and accelerated CEC loss in addition to the worldwide shortage of donor tissue drive clinicians to strive for surgical procedures that even more selectively remove only irreversibly diseased parts of the endothelial monolayer and—only where necessary—transplant healthy CECs.[3–5] The Descemet stripping only (DSO) procedure offers a first approach and includes surgical removal of the central 4 mm of DM and adjacent corneal endothelium without subsequent corneal endothelial transplantation. However, DSO delivers inconsistent postoperative results and endothelial regeneration cannot be accomplished in all patients.[6–9] Patient characteristics that determine postoperative outcome remain elusive.[10] In order to optimize and establish appropriate novel procedures, diseased parts of both DM and endothelium must be made clearly identifiable.

An improved understanding of CEC density and its correlation to the pathology of DM in advanced FECD will be necessary. Early elaborate studies have provided a detailed description of the DM ultrastructure: the normal DM is composed of a prenatally developed anterior banded layer (ABL) and a posterior nonbanded layer constantly secreted by CECs throughout lifetime.[11] This stratification is

0002-9394/$36.00
https://doi.org/10.1016/j.ajo.2020.09.030

subject to significant changes in FECD with additional layers of ECM secreted by a diseased endothelium leading to a thickening of DM and the formation of posterior excrescences, called guttae.[1,12–14] This abnormal stratification of DM also brings about alterations of ECM composition, which was reported to be rich in ECM proteins including collagens I, III, and IV (COL I, COL III, and COL IV), particularly in advanced stages of FECD.[15,16]

To further improve the detection of diseased endothelium as a basis for optimized diagnosis and individualized treatment in FECD, the present study aimed to characterize CEC density as a measure of endothelium viability in correlation to changes of collagen composition of DM and investigated if such changes of DM may be imaged by slit-lamp biomicroscopy.

METHODS

• **SUBJECTS:** In this prospective, observational consecutive case series, explanted Descemet endothelium complexes (DECs, corneal endothelium, and adherent DM) were retrieved from patients undergoing DMEK or DMEK with phacoemulsification and intraocular lens implantation (triple DMEK) for advanced FECD (and cataract) at the Department of Ophthalmology, University of Cologne, Germany (Supplemental Figure S1, A and B). Formal approval to conduct this study was obtained from the Ethics Committee of the University of Cologne (14-248). Written informed consent has been obtained from all participants for the treatment and participation in the research. The research adhered to the tenets of the Declaration of Helsinki.

Routine preoperative clinical examination included slit-lamp biomicroscopy, funduscopy, and Scheimpflug imaging (Pentacam HR; Oculus, Wetzlar, Germany). Diagnosis of FECD was confirmed and modified Krachmer grading was performed by 1 of 3 corneal specialists (B.B., C.C., M.M.) as previously described.[17,18] Inclusion criteria were advanced late-onset FECD (modified Krachmer grade 5 or 6) as determined by slit-lamp biomicroscopy. Exclusion criteria were corneal disease other than FECD, diabetes, ocular surgery other than cataract surgery, and systemic infectious disease.

Specular microscopy was not part of our protocol because previous studies had shown that no reliable images can be acquired by specular microscopy in advanced FECD eyes with significant corneal edema.[19,20]

• **TISSUE SAMPLING AND IMMUNOFLUORESCENCE STAINING:** Patients underwent (triple) DMEK surgery as previously described in detail with Descemetorhexis performed at standard size 8 mm.[21] Explanted DECs were immediately immersed and fixed in 4% paraformaldehyde and stored at 4 C.[21]

For immunofluorescence staining, DECs were washed and permeabilized twice with phosphate-buffered saline (PBS) with 0.1% 1M magnesium chloride, 0.01% 1M calcium chloride, and 0.1% Triton X-100 (PBS^{T++}) followed by additional washing with PBS^{T++} containing 50 mM ammonium chloride. Blocking for nonspecific binding sites was performed for 1 h at room temperature with 1% bovine serum albumin in PBS^{T++}.

Primary antibodies used for single immunofluorescence staining were rabbit polyclonal anti–COL I (1:500 dilution, catalog no. ab34710; Abcam, Cambridge, UK), rabbit polyclonal anti–COL III (1:400 dilution, catalog no. ab7778; Abcam), and mouse monoclonal anti–COL IV (1:100 dilution, catalog no. ab6311; Abcam). DECs were incubated at 4 C overnight in the primary antibody. DECs were washed 3 times with 0.2% bovine serum albumin in PBS^{T++} and incubated for 1 h at room temperature in secondary antibody. Secondary antibodies used were goat Cy3 antirabbit (1:100 dilution, catalog no. 111-165-045; Dianova, Hamburg, Germany) and rabbit Cy3 antimouse (1:100 dilution, catalog no. 315-165-003; Dianova). DECs were subsequently washed 3 times with 0.2% bovine serum albumin in PBS^{T++}. Nuclei were counterstained with 4′, 6-diamidino-2-phenylindole and DECs were flat mounted for optimized assessment. Negative control was performed using secondary antibody only (Supplemental Figure S1, C).

• **IMAGE ACQUISITION AND DATA ANALYSIS:** To characterize changes in collagen composition and related changes in CEC density we followed a stepwise approach. Images of complete stained and flat mounted DECs were acquired using fluorescence microscopes BX53/BX63 (Olympus, Hamburg, Germany) at ×20 magnification. Image analysis was performed using the open source software platform Fiji.[22]

In a first step, the border of flat mounted DECs as well as collagen-positive (positive region of interest [ROI^+]) and collagen-negative areas (negative ROI^-) were identified, marked, and their respective surface and the maximum diameter of ROI^+ were calculated using Fiji (Supplemental Figure S1, D). DECs from patients with FECD without ROI^+ were used as control subjects. A central circular 10-mm^2 area (corresponding to the mean ROI^+ area of COL I–, COL III–, and COL IV–positive DECs) was defined as $ROI^{control\ central}$ and the peripheral part defined as $ROI^{control\ peripheral}$. Areas including ≥2 layers of DEC or missing parts of DEC were excluded from the evaluation.

In a second step, CEC nuclei were identified using the Fiji function "Analyze Particles." CEC density per square millimeter was calculated per ROI area, respectively, counting 1 CEC per identified corneal endothelial nucleus.

TABLE. Demographic Data

	COL I	COL III	COL IV	Total
Eyes, n	19	18	13	50
Age (y), mean ± standard deviation	69.6 ± 9.4	65.7 ± 8.4	63.8 ± 8.5	66.7 ± 9
Female, n (%)	11 (57.9)	12 (66.7)	8 (61.5)	31 (62)
Pseudophakic, n (%)	7 (36.8)	4 (22.2)	4 (30.8)	15 (30)
Central corneal thickness (μm), mean ± standard deviation	645.7 ± 57.3	641.6 ± 70.2	637 ± 61.3	642.1 ± 62
Fibrillar layer positive, n (%)	16 (84.2)	15 (83.3)	11 (84.6)	42 (84)

COL = collagen.

In a third step, changes of CEC density at the border of ROI^+ to ROI^- were examined in collagen positive DECs to objectivate the observed decline. CEC density was determined at the 12, 3, 6, and 9 o'clock position over a rectangular area of 0.2 mm × 0.8 mm subdivided into 4 squares with 2 squares positioned in ROI^+ (squares 1 and 2) and ROI^- (squares 3 and 4), respectively (Supplemental Figure S1, D). This step was essential to describe and objectify the decline in CEC density at the ROI^+-to-ROI^-border.

The LSM 880 confocal microscope (Zeiss, Oberkochen, Germany) was used to acquire Z-stack images at ×63 magnification of stained DECs to analyze the collagen expression within the stratification of DM layer in cross-sections (Supplemental Figure S1, E).

• **SLIT-LAMP BIOMICROSCOPY OF ROI^+ AREAS:** Analysis of the first 32 patients provided evidence for increased loss of CEC density in ROI^+ areas ex vivo. This prompted us to investigate in an additional 18 consecutive patients if an ROI^+ morphologic correlate would also be detectable in vivo. Detailed preoperative slit-lamp biomicroscopic images were taken at ×16 magnification and focused on the posterior corneal surface (Supplemental Figure S1, F). For optimized imaging the pupil was dilated and used as a homogeneous background to display the fine grayish and partially with pigment interspersed structure of the assumed ROI^+-correlate. Slit-lamp biomicroscopic images and histologic images were thoroughly compared to identify common morphologic details displayed by both modalities. For additional quantitative analysis, the maximum diameter ($d_{SL\ max}$) of the assumed ROI^+ correlate was determined by slit-lamp biomicroscopy using the slit-beam and compared with the maximum diameter ($d_{IF\ max}$) of the ROI^+ determined by immunofluorescence microscopy using Fiji.

• **STATISTICS:** Graph Pad Prism for Windows (version 8.4; GraphPad Software, San Diego, California, USA) was used to perform statistical analysis. The Shapiro–Wilk test was used to determine the Gaussian distribution of the measured values. A 2-tailed Student *t* test was performed for parametric datasets and a Mann–Whitney *t* test was used for nonparametric datasets. Statistical significance of independent groups was verified using ordinary 1-way analysis of variance followed by Tukey multiple comparison test and Kruskal Wallis test followed by Dunn multiple comparison test in case of non-Gaussian distribution. Correlation analysis was performed using 2-tailed Pearson correlation or Spearman correlation for nonparametric datasets ($r = 0$ to 1 positive correlation, $r = 0$ no correlation, $r = 0$ to -1 inverse correlation). All data are presented as mean values with standard deviation ($P > .05$; $^*P \leq .05$; $^{**}P \leq .01$; $^{***}P \leq .001$; $^{****}P \leq .0001$).

RESULTS

THE DECS OF A TOTAL OF 50 EYES OF 50 PATIENTS WITH advanced FECD were included in this study. Demographic data are presented in Table. Gender distribution showed female predominance recapitulating gender distribution in FECD.

• **COLLAGEN EXPRESSION:** A proportion of 84% (42/50) of all DEC flat mounts showed clearly delimitable coherent COL I, COL III, or COL IV staining of the central or paracentral area. Collagen-positive stained areas were referred to as ROI^+ whereas the surrounding peripheral area without staining was referred to as ROI^- (Supplemental Figure S1, D). A ROI^+ was detectable in 84.2% (16/19) of DECs stained for COL I, in 83.3% (15/18) of DECs stained for COL III, and in 84.6% (11/13) of DECs stained for COL IV, respectively (Figure 1). There was no significant difference in the presence of a ROI^+ between DECs stained for COL I, COL III, and COL IV ($P > .99$).

Within COL I, COL III, and COL IV ROI^+, cross-sectional Z-stack analysis of DECs revealed deposits of respective collagens at the posterior surface of DM.

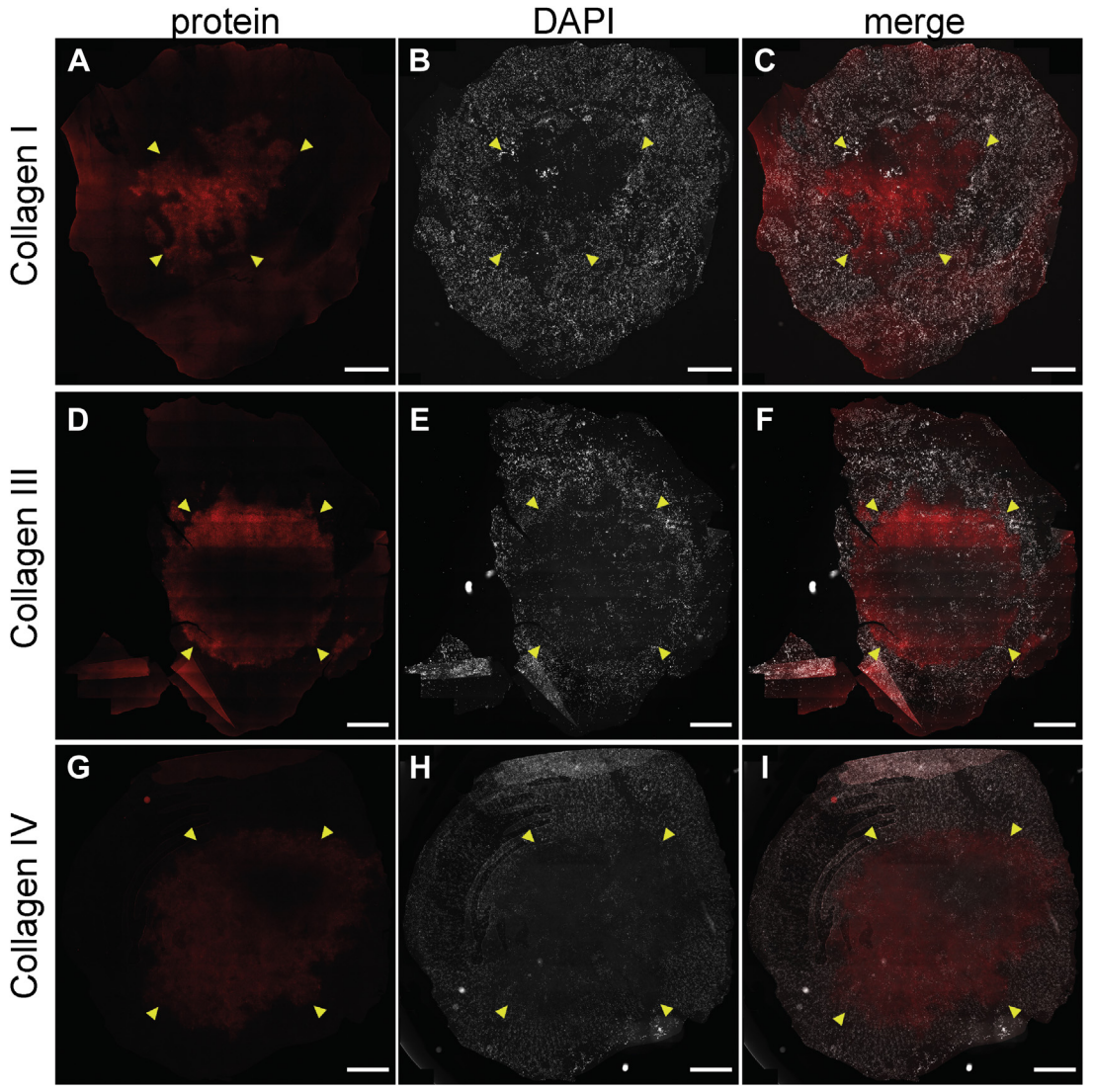

FIGURE 1. Microscopic analysis of Descemet endothelium complex (DEC) flat mounts from patients with advanced Fuchs endothelial corneal dystrophy after immunofluorescence staining: DECs were stained for collagen I (A, red), collagen III (A, red), and collagen IV (G, red). Nuclei of corneal endothelial cells were counterstained with 4′,6-diamidino-2-phenylindole (DAPI; B, E, and H, white). Microscopic analysis shows central collagen staining (A, D, and G, yellow closed triangles) and concomitant loss of corneal endothelial cells (B, E, and H, yellow closed triangles). Merged collagen and DAPI images are shown in (C), (F), and (I) (×20 magnification; bar = 1 mm).

Collagen deposits bury guttae in an additional layer of extracellular matrix (Figure 2) corresponding to a fibrillar layer (FL) as described in previous late-onset FECD studies.[14–16,23–25] No such deposits were observed in the ROI^- of respective samples (Figure 2).

• **SURFACE AREA:** The mean surface area of all ROI^+ was 10 mm^2 ± 6 mm^2. The mean ROI^+ surface area was 8.2 mm^2 ± 5.8 mm^2 in DECs stained for COL I, 10.2 mm^2 ± 5.9 mm^2 in DECs stained for COL III, and 12.5 mm^2 ± 6.1 mm^2 in DECs stained for COL IV. There was no significant difference in the ROI^+ surface area between DECs stained for COL I, COL III, and COL IV ($P > .05$, respectively).

• **CORNEAL ENDOTHELIAL CELL DENSITY:** In DECs with detectable ROI^+, the total CEC density was 747 ± 299 (n = 42). In DECs without detectable ROI^+, the total CEC density was 1028 ± 503 (n = 8). There was a significant difference in total CEC density between DECs with and without detectable ROI^+ ($P = .04$).

In DECs with detectable ROI^+, the mean ROI^+ CEC density compared with the ROI^- CEC density was 381 ± 226 and 842 ± 314 (n = 42; $P < .0001$), corresponding

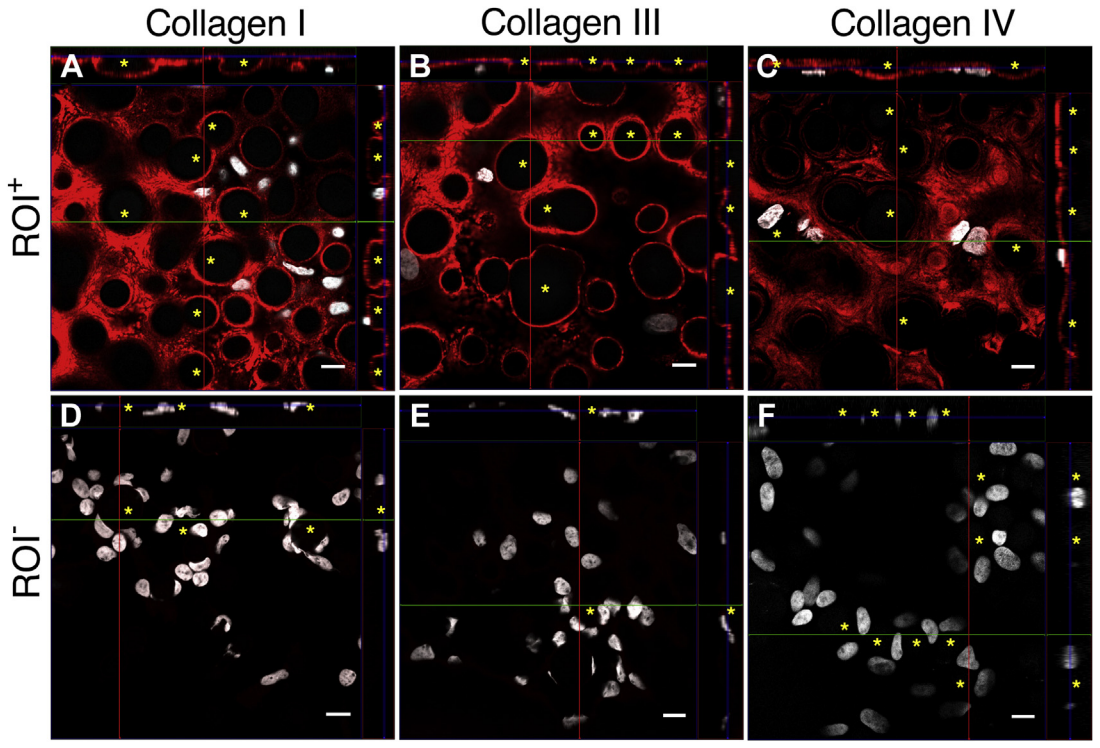

FIGURE 2. Microscopic (confocal Z-stack) analysis of Descemet endothelium complex (DEC) flat mounts from patients with advanced Fuchs endothelial corneal dystrophy after immunofluorescence staining: DECs were stained for collagen I (A and D, red), collagen III (B and E, red), and collagen IV (C and F, red). Nuclei were counterstained with 4′,6-diamidino-2-phenylindole (DAPI; white). Respective subfigures show en face section of DECs. Cross sections as marked by horizontal green and vertical red lines within each en face section are shown at top and right margin of the same subfigure. Only guttae appearing in cross sections are marked (yellow asterisk). Microscopic analysis confirms collagen deposition at the posterior surface of Descemet membrane and corresponding to a fibrillar layer in the collagen-positive region of interest (ROI^+) (A, B, and C) whereas no such layer may be observed in collagen-negative ROI (ROI^-; D, E, and F). (Green line: X-Z axis; red line: Y-Z axis; blue line: Z-stack position; ×63 magnification; bar = 10 μm.)

to a relative decrease of CEC density in ROI^+ compared with ROI^- of 54.8%. In DECs without detectable ROI^+, the mean $ROI^{control\ central}$ CEC density compared with the $ROI^{control\ peripheral}$ CEC density was 972 ± 439 and 1047 ± 552 (n = 8; $P = .77$).

Comparing the CEC density of ROI^+ areas to the mean CEC density of $ROI^{control\ central}$ areas there was a significant difference ($P = .0003$). Comparing the CEC density of ROI^- areas to the mean CEC density of $ROI^{control\ peripheral}$ areas there was no significant difference ($P = .15$).

In DECs with detectable ROI^+, the ROI^+ CEC density compared with the ROI^- CEC density was 343 ± 171 and 753 ± 259 (n = 16; $P < .0001$) in DECs stained for COL I, 427 ± 325 and 807 ± 352 (n = 15; $P = .006$) in DECs stained for COL III, and 374 ± 110 and 1019 ± 285 (n = 11; $P < .0001$) in DECs stained for COL IV (Figure 3). This corresponds to a relative decrease of CEC density in ROI^+ compared with ROI^- of 54.4% (COL I), 47.1% (COL III), and 63.3% (COL IV), respectively. There was no significant difference in ROI^+ CEC density ($P > .99$) or ROI^- CEC density ($P > .05$) between DECs stained for COL I, COL III, and COL IV, respectively.

In DECs with detectable ROI^+, the decline of CEC density at the ROI^+ to ROI^- border was determined by analysis of CEC density in 4 squares equally arranged at both sides of the staining border at the 12, 3, 6, and 9 o'clock positions as described above (Supplemental Figure S1, D). Comparison of CEC density in these 4 squares demonstrated a steep and significant ($P < .0001$) decline from ROI^- to ROI^+ areas as shown in Figure 4.

• **CENTRAL CORNEAL THICKNESS AND CORRELATION ANALYSIS:** In DECs with detectable ROI^+, the central corneal thickness (CCT) was 645.7 μm ± 55.3 μm (n = 42). In DECs without detectable ROI^+, the CCT was 611.1 μm ± 88.4 μm (n = 8). There was no significant difference in CCT between DECs with and without detectable ROI^+ ($P = .15$). In DECs with detectable ROI^+, there was no significant correlation of CCT to the ROI^+ area ($r = -0.21$; $P = .18$), of CCT to total CEC density ($r = -0.06$; $P = .69$), or of CCT to CEC density of

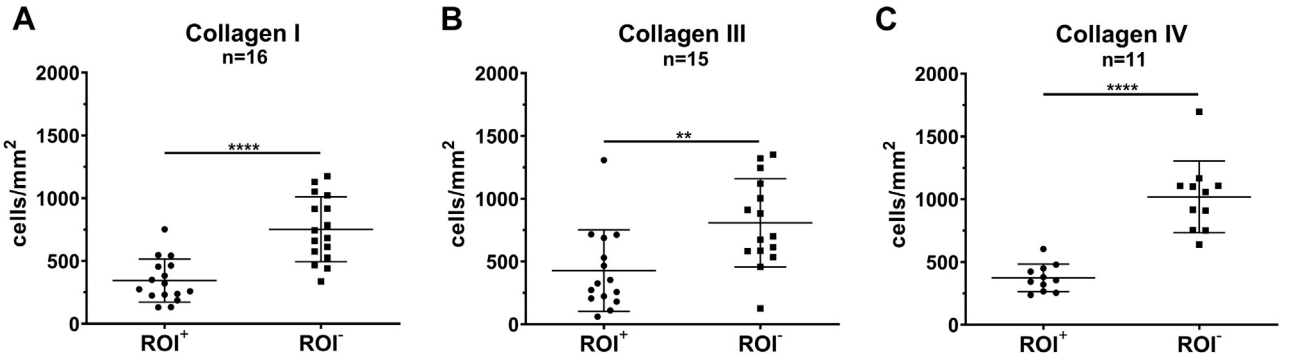

FIGURE 3. Corneal endothelial cell density in relation to collagen staining of Descemet endothelium complex: comparison of regions of interest (ROI) with (ROI^+) and without (ROI^-) collagen staining shows significantly reduced corneal endothelial cell density in ROI^+ exhibiting increased staining of collagen I (A), collagen III (B), and collagen IV (C), respectively. $^{**}P < .01$, $^{****}P < .0001$.

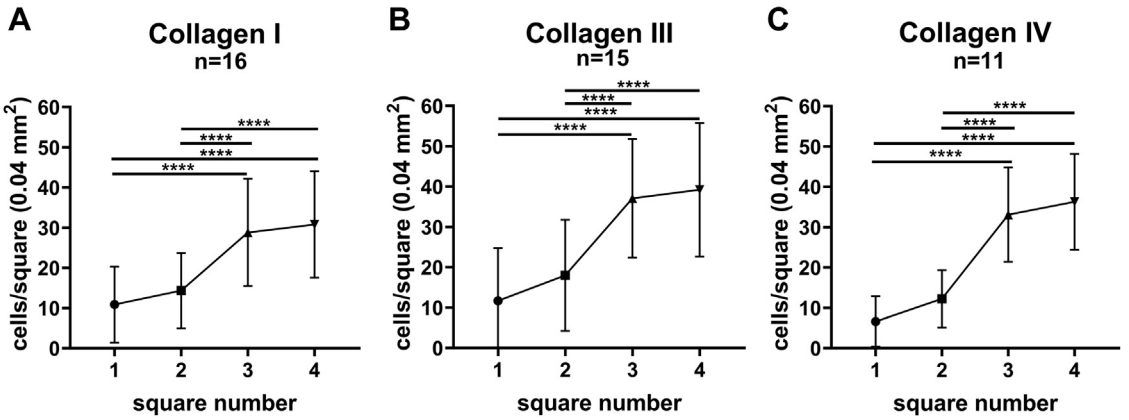

FIGURE 4. Decline of corneal endothelial cell density at the borderline between stained region of interest (ROI^+) and unstained ROI (ROI^-). Corneal endothelial density was determined in 4 squares equally arranged at both sides of ROI^+ to ROI^- borderline at the 12, 3, 6, and 9 o'clock positions (described in Supplemental Figure S1, D). Comparison of corneal endothelial cell density in these 4 squares shows a steep and significant decline from ROI^- to ROI^+ areas in collagen I (A), collagen III (B), and collagen IV (C) stained Descemet endothelium complexes. $^{****}P < .0001$.

ROI^- areas ($r = -0.05$; $P = .77$). However, there was a significant negative correlation of CCT to CEC density of ROI^+ ($r = -0.31$; $P = .045$). In DECs without detectable ROI^+, there was no significant correlation of CCT to total CEC density ($r = -0.6$; $P = .11$), of CCT to CEC density of $ROI^{control\ central}$ ($r = -0.64$; $P = .09$), or of CCT to CEC density of $ROI^{control\ peripheral}$ areas ($r = -0.58$; $P = .13$).

• **COMPARISON OF PHAKIC AND PSEUDOPHAKIC FECD EYES:** An ROI^+ area was detectable in 83% (29/35) of all patients with phakic FECD (phFECD) and in 87% (13/15) of all patients with pseudophakic FECD (psphFECD) and there was no significant difference in the detection of an ROI^+ area between patients with phFECD and those with psphFECD ($P > .99$). There was no significant difference in the ROI^+ area comparing phFECD (11.14 $mm^2 \pm 6\ mm^2$; n = 29) and psphFECD (7.9 $mm^2 \pm 6\ mm^2$; n = 13; $P = .09$) eyes. However, there was a significantly higher total CEC density in phFECD eyes (826 ± 306; n = 29) compared with psphFECD eyes (571 ± 192; n=13; $P = .009$). This was also reflected by a significantly higher ROI^+ CEC density in phFECD eyes (427 ± 245; n = 29) compared with psphFECD eyes (279 ± 134; n = 13; $P = .05$) and a significantly higher ROI^- CEC density in phFECD eyes (934 ± 315; n = 29) compared with psphFECD eyes (636 ± 198; n = 13; $P = .003$). The CCT showed no significant difference comparing phFECD eyes (642 μm ± 58 μm) and psphFECD eyes (654μ ± 51μm, $P = .53$).

• **SLIT-LAMP BIOMICROSCOPY OF ROI^+ AREAS:** Subgroup analysis (18 patients) by slit-lamp biomicroscopy showed

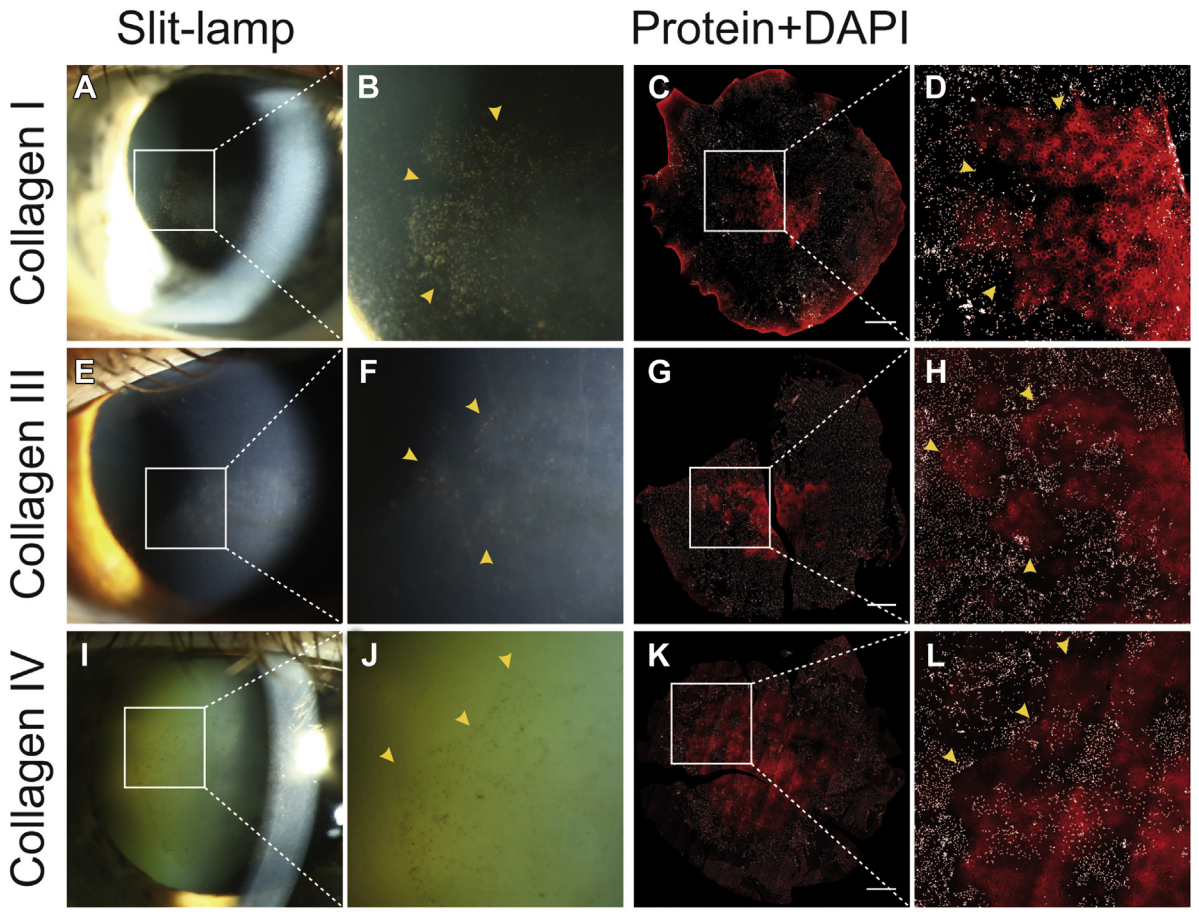

FIGURE 5. Slit-lamp biomicroscopy and immunofluorescence staining of the fibrillar layer in advanced Fuchs endothelial corneal dystrophy: slit-lamp biomicroscopy of the posterior corneal surface shows gray deposits with pigment inclusions at the posterior stromal surface (A, B, E, F, I, and J). After Descemet membrane endothelial keratoplasty surgery, explanted Descemet endothelium complexes (DECs) were stained for collagen I (C and D, red), collagen III (G and H, red), and collagen IV (K and L, red) and nuclei were counterstained with 4′,6-diamidino-2-phenylindole (white). Morphologic characteristics of the fibrillar layer observed in slit-lamp biomicroscopy (B, F, and J, yellow closed triangles) are recapitulated in explanted DECs after immunofluorescence staining (D, H, and L, yellow closed triangles; ×16 magnification; bar = 1 mm).

gray deposits with or without pigment inclusions at the posterior corneal surface in 16 of 18 (88.9%) patients. These deposits exhibited characteristic morphologic features of the ROI^+ detected by immunofluorescence staining in the corresponding DECs (Figure 5). No deposits were found by slit-lamp biomicroscopy in 2 (11.1%) patients and the corresponding DECs also showed no collagen deposits by immunofluorescence analysis. Maximum diameter of deposits measured by slit-lamp biomicroscopy was $d_{SL\ max}$ = 4.1 mm ± 0.9 mm and maximum diameter of the corresponding ROI^+ determined by immunofluorescence microscopy was $d_{IF\ max}$ 4.7 mm ± 1.1 mm (n = 16; P = .1; Figure 6). There was a significantly positive correlation between $d_{SL\ max}$ and $d_{IF\ max}$ (r = 0.76; P = .001). There was no significant difference in $d_{SL\ max}$ and $d_{IF\ max}$ for COL I (n = 5; P = .8), COL III (n = 7; P = .11), and COL IV (n = 4; P = .17).

DISCUSSION

THE PRESENT STUDY SHOWS THAT GEOGRAPHIC SUBENDOthelial COL I–, COL III–, and COL IV–rich areas, corresponding to a FL of DM, are present underneath the central corneal endothelium of the majority (84%) of advanced FECD eyes and may be imaged by slit-lamp biomicroscopy in vivo. Moreover, it indicates for the first time that this FL corresponds to areas of pronounced loss of CECs with a steep decline in CEC density at its borders. In vivo imaging of the FL may provide a basis for more precise and individualized medical and surgical treatment of FECD in the future (Supplemental Figure S1, F).

The ABL of DM develops prenatally. Posteriorly located layers of ECM are secreted by the corneal endothelium throughout lifetime and represent a record of normal and pathologic events similar to tree rings describing varying

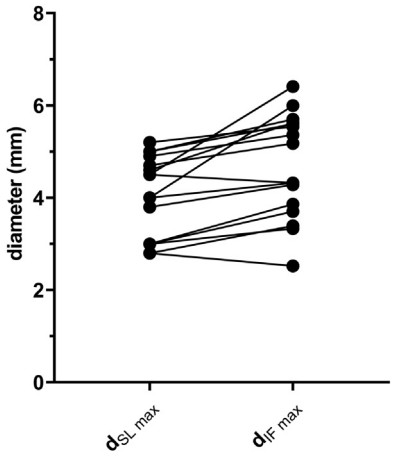

FIGURE 6. Maximum diameter of fibrillar layer: measured by slit-lamp biomicroscopy ($d_{SL\ max}$) or by immunofluorescence staining and microscopy ($d_{IF\ max}$).

climatic conditions during growth.[12] The DM of patients with FECD exhibits a normal ABL.[12,26,27] The posterior nonbanded layer is dilute or nonexistent.[12,26,27] An additional posterior banded layer forms posterior excrescences (guttae) and leads to a significant thickening of DM.[12,14,26,27] In advanced stages of the disease, an FL is secreted by a decompensated and stressed corneal endothelium and buries the guttae in a collagen-rich matrix including COL I, COL III, and COL IV.[12,15,16,27] This FL corresponds to the subendothelial ROI^+ collagen deposits described in the present study.

A recent study classified the ultrastructure of FECD DM and differentiated 3 types: type I showing an ABL, a posterior nonbanded layer, and a posterior banded layer, type II showing an additional FL, and type III showing a FL burying the first layer of guttae and a second additional layer of guttae protruding like type I FECD DM.[23] Bourne and associates[12] hypothesized that corneal decompensation is paralleled by increased leakage through the corneal endothelium into DM causing the formation of a loose FL rather than a compact collagenous layer.[12] This group was able to show that an increased FL thickness correlates with greater stromal and epithelial edema in advanced FECD.[12] They found an FL in 7 of 11 (64%) corneas of patients with FECD undergoing penetrating keratoplasty[12]; Yuen and associates[28] found an FL in 19 of 32 (59%) of patients with FECD.[28] The Krachmer grading of patients with FECD is not reported in these studies and corresponding deviations in the selection of patients may be responsible for the higher percentage of FL–positive cases (84%) in our study. Although there was a lower CEC density in pseudophakic compared with phakic FECD eyes in our study, our investigations did not provide any evidence that cataract surgery affects the size of the FL.

The location of deposits and expression of COL I, COL III, and COL IV in our study are compatible with previous descriptions of the FL in late-onset FECD corneas and suggest an endothelial or myofibroblast origin.[15,16,24,25,29] Since structural and compositional changes in the FECD DM affect cell behavior and may cause pathology, a primary pathogenetic role of the FL deposits in terms of an ECM-related toxic microenvironment needs to be considered.[23,30–32] In addition to the observed focal loss of CEC density, this would suggest that complete removal of the FL may be advantageous in procedures such as DSO. Interestingly, 33.3% (14/42) of DECs in our study exhibited an FL surface area of $>12.56\ mm^2$ and DSO with 4-mm standard diameter (and $12.56\ mm^2$ surface area) would not have led to full removal of these FL.

Clinically, an FL may be observed in advanced cases of FECD by slit-lamp biomicroscopy as central, gray deposits at the posterior stromal surface (Figure 5). These deposits often exhibit pigment inclusions, and our results indicate that borders and diameters of these deposits identified by slit-lamp biomicroscopy match borders identified by immunofluorescence (Figures 5 and 6).

Imaging, measurement, and marking of the FL area in vivo may be further optimized in the future by new high-resolution modalities such as optical coherence microscopy.

Building on such optimized imaging, future studies will investigate in more detail if the presence of an FL should be integrated into new clinical FECD classification systems.[33] This may seem reasonable because the FL is differentiated from "confluent guttae" as posterior layer embedding guttae rather than being part of their ultrastructure.[17,18] In our study, there was a significantly lower total CEC density in DECs with detectable FL compared with DECs without detectable FL. This further supports the results of previous studies showing that the incidence and the thickening of a FL may be associated with corneal decompensation occurring in more advanced cases of FECD and advocating for a progression of the FL over time.[12]

From a surgical point of view, identification of the FL may offer the opportunity to identify and selectively remove and replace particularly affected areas of the FECD endothelium. A study investigating CEC cultures from DECs of patients with FECD demonstrated that absence of a FL favored the successful culture of FECD cells.[34] In this regard, it will be interesting to see whether the presence of an FL affects regeneration of the endothelium after DMEK or DSO and whether individualized removal only of the most affected FL area in advanced FECD offers advantages over the Descemetorhexis of standard shape and size in the context of procedures like DSO, mini-, hemi-, or quarter-DMEK and novel treatments like corneal endothelial cell injection with rho-associated protein kinase inhibitor supplementation.[10,35–37] Large denuded areas without CECs were observed overlying the FL (Figures 1 and 5), and future studies will show if the FL can be intraoperatively identified using dyes such as Trypan blue.

Delineation of an FL in advanced FECD may also bring about new aspects for molecular studies investigating the pathogenesis of FECD: While fibrotic changes of the FL area rather mark late stages of FECD, early alterations of FECD pathology would be more likely to be found outside this area in the corneal endothelial periphery.

The present study is limited by the investigation of CEC density ex vivo and artificial changes of CEC density in context of the tissue sampling, the immunofluorescence staining process or evaluation have to be ruled out by future in vivo analyses. An FL-like secretion of ECM by stressed CECs was previously described in the context of other advanced corneal endothelial disorders such as pseudophakic or aphakic bullous keratopathy or pseudoexfoliation keratopathy.[28,38] Therefore, we cannot anticipate the observed FL-related loss of CEC density to be an FECD-specific effect.

In conclusion, the present study provides evidence that an FL defined as clearly demarcated subendothelial COL I–, COL III–, and COL IV–rich areas of variable size marks areas of pronounced loss of CECs in advanced FECD and that this FL may be imaged by slit-lamp biomicroscopy in vivo.

ALL AUTHORS HAVE COMPLETED AND SUBMITTED THE ICMJE FORM FOR DISCLOSURE OF POTENTIAL CONFLICTS OF INTEREST. Funding/Support: Supported by the German Research Foundation (FOR2240 to T.C., L.M.H., and C.C.; CL 751/1-1 to T.C.; HE 6743/3-1 and HE 6743/3-2 to L.M.H.; CU 47/6-1, CU 47/9- 1, and CU 47/12-1 to C.C., and MA 5110/5-1 to M.M.), the FORTUNE Program University of Cologne (to M.M. and L.M.H.), the GEROK Program University of Cologne (to L.M.H.), EU COST BM1302 "Joining Forces in Corneal Regeneration" and EU COST ANIRIDIA (to C.C., B.B., and S.S.), the Dr Gabriele Lederle Foundation, Taufkirchen (to L.M.H.), the Brigitte and Dr Konstanze Wegener foundation (to L.M.H.), the Marie-Louise Geissler foundation (to L.M.H.), EU Arrest Blindness (to C.C.), and EU EFRE NRW (to S.S.). Financial Disclosures: All authors indicate no conflicts of interest. All authors attest that they meet the current ICMJE criteria for authorship.

Acknowledgments: Confocal microscopy was conducted at the Department for Anatomy, University of Cologne, Germany. We thank Professor Wodarz and colleagues for their support.

REFERENCES

1. Matthaei M, Hribek A, Clahsen T, et al. Fuchs endothelial corneal dystrophy: clinical, genetic, pathophysiologic, and therapeutic aspects. *Annu Rev Vis Sci* 2019;5:151–175.
2. Gain P, Jullienne R, He Z, et al. Global survey of corneal transplantation and eye banking. *JAMA Ophthalmol* 2016;134(2):167–173.
3. Schrittenlocher S, Schaub F, Hos D, et al. Evolution of consecutive Descemet membrane endothelial keratoplasty outcomes throughout a 5-year period performed by two experienced surgeons. *Am J Ophthalmol* 2018;190:171–178.
4. Hos D, Tuac O, Schaub F, et al. Incidence and clinical course of immune reactions after Descemet membrane endothelial keratoplasty: retrospective analysis of 1000 consecutive eyes. *Ophthalmology* 2017;124(4):512–518.
5. Hos D, Matthaei M, Bock F, et al. Immune reactions after modern lamellar (DALK, DSAEK, DMEK) versus conventional penetrating corneal transplantation. *Prog Retin Eye Res* 2019;73:100768.
6. Arbelaez JG, Price MO, Price FW Jr. Long-term follow-up and complications of stripping descemet membrane without placement of graft in eyes with Fuchs endothelial dystrophy. *Cornea* 2014;33(12):1295–1299.
7. Borkar DS, Veldman P, Colby KA. Treatment of Fuchs endothelial dystrophy by Descemet stripping without endothelial keratoplasty. *Cornea* 2016;35(10):1267–1273.
8. Bleyen I, Saelens IE, van Dooren BT, et al. Spontaneous corneal clearing after Descemet's stripping. *Ophthalmology* 2013;120(1):215.
9. Ham L, Dapena I, Moutsouris K, Melles GR. Persistent corneal edema after descemetorhexis without corneal graft implantation in a case of fuchs endothelial dystrophy. *Cornea* 2011;30(2):248–249.
10. Garcerant D, Hirnschall N, Toalster N, et al. Descemet's stripping without endothelial keratoplasty. *Curr Opin Ophthalmol* 2019;30(4):275–285.
11. Wilson SE, Bourne WM. Fuchs' dystrophy. *Cornea* 1988;7(1):2–18.
12. Bourne WM, Johnson DH, Campbell RJ. The ultrastructure of Descemets membrane .3. Fuchs dystrophy. *Arch Ophthalmol* 1982;100(12):1952–1955.
13. Waring GO 3rd. Posterior collagenous layer of the cornea. Ultrastructural classification of abnormal collagenous tissue posterior to Descemet's membrane in 30 cases. *Arch Ophthalmol* 1982;100(1):122–134.
14. Iwamoto T, Devoe AG. Electron microscopic studies on Fuchs combined dystrophy .1. Posterior portion of cornea. *Invest Ophthalmol Vis Sci* 1971;10(1):9–28.
15. Weller JM, Zenkel M, Schlotzer-Schrehardt U, et al. Extracellular matrix alterations in late-onset Fuchs' corneal dystrophy. *Invest Ophthalmol Vis Sci* 2014;55(6):3700–3708.
16. Matthaei M, Hu J, Kallay L, et al. Endothelial cell microRNA expression in human late-onset Fuchs' dystrophy. *Invest Ophthalmol Vis Sci* 2014;55(1):216–225.
17. Krachmer JH, Purcell JJ Jr, Young CW, et al. Corneal endothelial dystrophy. A study of 64 families. *Arch Ophthalmol* 1978;96(11):2036–2039.
18. Louttit MD, Kopplin LJ, Igo RP Jr, et al. A multicenter study to map genes for Fuchs endothelial corneal dystrophy: baseline characteristics and heritability. *Cornea* 2012;31(1):26–35.
19. Ong Tone S, Jurkunas U. Imaging the corneal endothelium in Fuchs corneal endothelial dystrophy. *Semin Ophthalmol* 2019;34(4):340–346.
20. Laing RA, Leibowitz HM, Oak SS, et al. Endothelial mosaic in Fuchs' dystrophy. A qualitative evaluation with the specular microscope. *Arch Ophthalmol* 1981;99(1):80–83.

21. Matthaei M, Bachmann B, Siebelmann S, et al. Technique of Descemet membrane endothelial keratoplasty (DMEK): Video article [in German]. *Ophthalmologe* 2018;115(9): 778–784.
22. Schindelin J, Arganda-Carreras I, Frise E, et al. Fiji: an open-source platform for biological-image analysis. *Nat Methods* 2012;9(7):676–682.
23. Xia D, Zhang S, Nielsen E, et al. The ultrastructures and mechanical properties of the Descement's membrane in Fuchs endothelial corneal dystrophy. *Sci Rep* 2016;6:23096.
24. Kay ED, Cheung CC, Jester JV, et al. Type I collagen and fibronectin synthesis by retrocorneal fibrous membrane. *Invest Ophthalmol Vis Sci* 1982;22(2):200–212.
25. Gottsch JD, Zhang C, Sundin OH, et al. Fuchs corneal dystrophy: aberrant collagen distribution in an L450W mutant of the COL8A2 gene. *Invest Ophthalmol Vis Sci* 2005;46(12): 4504–4511.
26. Adamis AP, Filatov V, Tripathi BJ, Tripathi RC. Fuchs endothelial dystrophy of the cornea. *Surv Ophthalmol* 1993;38(2): 149–168.
27. Waring GO 3rd, Bourne WM, Edelhauser HF, et al. The corneal endothelium. Normal and pathologic structure and function. *Ophthalmology* 1982;89(6):531–590.
28. Yuen HK, Rassier CE, Jardeleza MS, et al. A morphologic study of Fuchs dystrophy and bullous keratopathy. *Cornea* 2005;24(3):319–327.
29. Heindl LM, Schlotzer-Schrehardt U, Cursiefen C, et al. Myofibroblast metaplasia after descemet membrane endothelial keratoplasty. *Am J Ophthalmol* 2011;151(6): 1019–1023.e2.
30. Borderie VM, Baudrimont M, Vallee A, Ereau TL, Gray F, Laroche L. Corneal endothelial cell apoptosis in patients with Fuchs' dystrophy. *Invest Ophthalmol Vis Sci* 2000;41(9): 2501–2505.
31. Kocaba V, Katikireddy KR, Gipson I, et al. Association of the gutta-induced microenvironment with corneal endothelial cell behavior and demise in Fuchs endothelial corneal dystrophy. *JAMA Ophthalmol* 2018;136(8):886–892.
32. Rizwan M, Peh GS, Adnan K, et al. In vitro topographical model of Fuchs dystrophy for evaluation of corneal endothelial cell monolayer formation. *Adv Healthc Mater* 2016;5(22): 2896–2910.
33. Horstmann J, Schulz-Hildebrandt H, Bock F, et al. Label-free in vivo imaging of corneal lymphatic vessels using microscopic optical coherence tomography. *Invest Ophthalmol Vis Sci* 2017;58(13):5880–5886.
34. Zaniolo K, Bostan C, Rochette Drouin O, et al. Culture of human corneal endothelial cells isolated from corneas with Fuchs endothelial corneal dystrophy. *Exp Eye Res* 2012; 94(1):22–31.
35. Kinoshita S, Koizumi N, Ueno M, et al. Injection of cultured cells with a ROCK inhibitor for bullous keratopathy. *N Engl J Med* 2018;378(11):995–1003.
36. Birbal RS, Hsien S, Zygoura V, et al. Outcomes of hemi-Descemet membrane endothelial keratoplasty for Fuchs endothelial corneal dystrophy. *Cornea* 2018;37(7):854–858.
37. Zygoura V, Baydoun L, Ham L, et al. Quarter-Descemet membrane endothelial keratoplasty (Quarter-DMEK) for Fuchs endothelial corneal dystrophy: 6 months clinical outcome. *Br J Ophthalmol* 2018;102(10):1425–1430.
38. Naumann GO, Schlotzer-Schrehardt U. Keratopathy in pseudoexfoliation syndrome as a cause of corneal endothelial decompensation: a clinicopathologic study. *Ophthalmology* 2000;107(6):1111–1124.